

A Density Matrix Renormalization Group study of Excitons in Dendrimers

M.A. Martín-Delgado*, J. Rodríguez-Laguna* and G. Sierra*

*Departamento de Física Teórica I, Universidad Complutense. 28040 Madrid, Spain.

*Instituto de Matemáticas y Física Fundamental, C.S.I.C., Madrid, Spain.

We introduce the density matrix renormalization group (DMRG) method as an efficient computational tool for one-exciton approximations with off-diagonal disorder. This method allows us to reduce the computational effort by targetting only a few low-lying eigenstates at each statistical samplings, in contrast to the exact diagonalization methods that compute the whole spectrum. As an application of the method, we study excitons in two families of branched molecules called dendrimers using a recently introduced simple model. We compute the absorption peaks for these dendrimers varying their generation number g and number of wedges w .

PACS numbers: 75.10.-b, 05.50.+q, 71.35.Cc

I. INTRODUCTION

Dendrimers are large, highly branched polymers [1] (see Fig.1). Some individual dendrimer molecules exceed ten nanometers in diameter. These hyperbranched molecules are composed of a central core to which repetitive dendritic branches are attached [2]. Dendrimers have several distinctive architectural components. Some of them are: i) an initial core also called *focal point*; ii) interior layers called *generations*, composed of repeating units radially attached one after another. This number determines the branch length; iii) the degree of *connectivity* of each single molecule in a given site of the macromolecule, i.e., the number of nearest-neighbours for a given site in the associated lattice model. This can vary from site to site; iv) the number of initial strands attached to the focal point can be made variable and leads to various separated branches that are called *wedges* or *lobes*. In other words, this is the core multiplicity. Thus, we can partially characterize the lattice model of a dendrimer using the notation

$$D(w, c, g; N) \quad (1)$$

to denote a dendrimer with w wedges, connectivity c , g generations and total number of sites N . The number of sites can be obtained from the previous data (w, g, c) . In the following we shall use this nomenclature and a planar representation of dendrimers (see Figs.2, 3). Particular examples of dendrimer lattices are a binary tree, a Bethe lattice or a Cayley tree.

The field of highly branched macromolecules can also be addressed from the viewpoint of polymer chemistry. We may classify polymers in two big groups: linear and branched polymers. Standard polymers elongate in a linear fashion [6], [7], [8], while the new dendritic polymers

are branched [3], [4], [5]. Dendritic polymers differ from linear polymers in that the latter consists of long chains of molecules, like coils, crisscrossing each other, while dendrimers have numerous chain-ends that can be functionalized. Because of this, dendritic molecules can be constructed with discrete domains having different properties. With a quite descriptive and friendly terminology, standard polymers are called “spaguetti-like” while dendrimers are called “meat-balls”.

The historical origins of dendrimers are in the quest for large, substrate-selective ligands, in which several research groups became interested yielding the synthesis of “tentacle” [9] and “octopus” [10, 11] molecular compounds, where long branches radiate from a central hub or a macrocycle. The first who reported a dendrimer synthesis was Fritz Vögtle in 1978 [12], introducing the concept of cascade reaction and cascade molecules, later known as dendrimers. Then, research groups led by Tomalia [13] and Denkewalter [14] devised routes whereby stepwise polymerisations could be

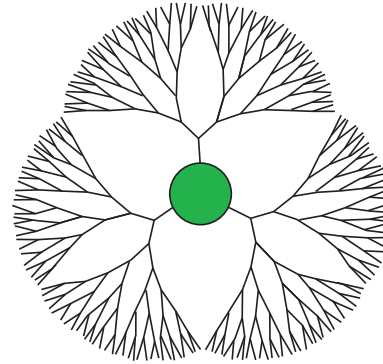


FIG. 1: A pictorial representation of a dendrimer with parameters $w = 3$, $c = 3$, $g = 7$.

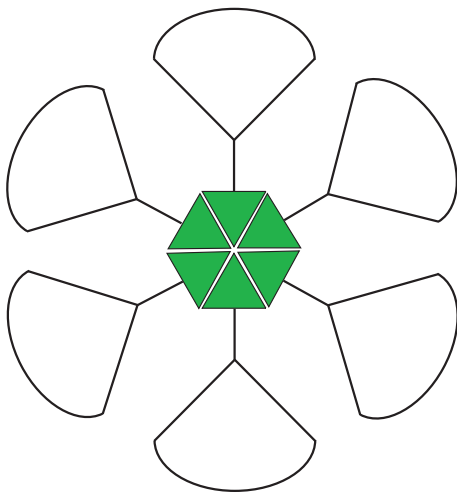


FIG. 2: Schematical representation of the wedges in a dendrimer with a core with 6 wedges. The wedges are assembled together as in the convergent method of synthesis [15].

achieved, producing highly branched polymers with extremely low polydispersities.

Dendrimers are constructed from branching units and a core. Their synthesis begins by attaching branched molecules to an initial core structure. Iterative polymerization of more branched molecules ultimately leads to a globular structure unable to accommodate further branching because of steric hindrance. Using multistep repetitive syntheses, chemists can construct the dendrimer layer by layer (generation by generation). This method is known as the “divergent method.” It was developed in 1978 by Fritz Vögtle. It is a difficult and tedious method for their synthesis, but it does allow exquisite tailoring of architectural features. Later, other alternative methods were proposed such as the “convergent method”, where dendrimers are built from the surface to the core, again using a reiterative sequence of reactions. This method was first introduced in [15].

Dendrimers may have a huge variety of constituent single molecular groups. Typically they contain carbon-based organic molecules such as polyamidoamines, aminoacids, DNA, and sugars, but also they are being constructed from organosilicons and organic/inorganic hybrids.

There are many examples of dendrimers whose constitutions have been designed with a purpose in mind. By an accurate choice of the building blocks to be used and specific functionalization in the periphery (external surface), many of their properties can be controlled such as the molecular weight, size, shape, chirality, density, viscosity, polarity, solubility, flexibility and surface chemistry of the resulting macromolecules. This leads to new materials with a great potential for future applications.

Interest in dendrimers has mushroomed after producing the wide range of structures that are known today,

and a great deal of potential applications for dendrimers have been proposed [3, 4, 5]. Among the many current and future applications we may cite drug delivery systems (in chemotherapy for instance), gene therapy, materials science, magnetic resonance imaging (MRI) contrast agents, molecular recognition, antiviral treatment, energy converters, etc. In material science, dendrimers may themselves act as building blocks in the fashioning of larger supramolecular structures.

Dendrimers include a great volume in relation to their molecular weight as a consequence of their dendritic structure. They may quite well be compared to bushes and trees in nature (see Fig.1). Cavities inside them can host guest species such as ions or another molecules. The potential of dendrimers in the fields of host-guest chemistry and nanotechnology relies on the subtle engineering of their architectures to pre-defined designs and taking advantage of these cavities inside them to encapsulate the guests.

Of all the many applications of dendrimers, we shall focus on their optical properties that confer them the potential applications as light-harvesting molecules, i.e., molecular antennas. There have been recent experiments addressing these issues by studying electron transfer in dendrimers of several types and their optical properties for absorption and emission of light [16].

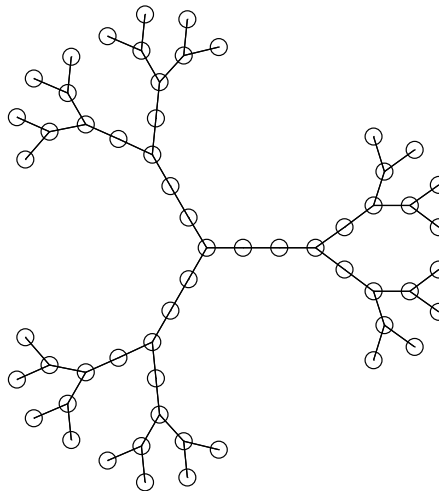


FIG. 3: An example of extended dendrimer with generation number $g = 4$ and wedges $w = 3$. At the ramification sites the coordination is $c = 3$ like in the compact dendrimers, while the new feature is the presence of intermediate sites at the legs with $c = 2$.

The functioning of dendrimers as single molecule photonic antenna systems relies on the large number of chain-ends that can be functionalized to absorbing photons at

the periphery and a subsequent efficient transfer of the absorbed energy to the center where a fluorescent trap or a laser dye can be placed at the dendritic core [16].

Following these experimental studies, we shall focus for the moment in two types of dendrimer families: *compact dendrimers* and *extended dendrimers*. They are shown in Fig.3. These are phenylacetylene dendrimers where at each node or site of the dendrimer lattice there are benzene molecules. Depending on the position of these benzenes, the branching of the site can be either two (*para* position) or three (*ortho* position). Compact dendrimers consists of three Cayley trees joined together at the focal point. This implies that the number of wedges is $w = 3$. All their sites exhibit ortho positions leading to a connectivity $c = 3$. The number of generations is variable. In [16] dendrimers up to generation 5 were studied. Thus, a compact dendrimer is a $D(3, 3, g; N(g))$ -dendrimer (1) with

$$N(g) = 1 + 3 \sum_{n=1}^g 2^{n-1} = 3 \times 2^g - 2. \quad (2)$$

This is an exponential growth. The first elements of this series are D4, D10, D22, D46, D94, etc. The experimental studies of [16] show that the electronic excitations of these fractal structures are of a localized nature.

Extended dendrimers have also a threefold symmetry around the focal point, but they have generation-dependent segments lengths. Namely, their sites can be of variable connectivity, either $c = 2$ (*para* position) or $c = 3$ (*ortho* position) depending on the generation. Thus, an extended dendrimer is a $D(3, [2, 3], g; N(g))$ -dendrimer (1) with

$$\begin{aligned} N(g) &= 1 + 3 \sum_{n=1}^g (g-n)2^{n-1} + 3 \cdot 2^{g-1} \\ &= 9 \times 2^{g-1} - 3g - 2, \end{aligned} \quad (3)$$

where the factor in (3) $l(g, n) \equiv g - n + 1$ ($n = 1, \dots, g$) is the length of each segment in the dendrimer. This is also an exponential growth. The first elements of this series are D4, D10, D25, D58, D127, etc.

Despite this small difference in the structure of extended dendrimers, it has important physical consequences which have been reported experimentally [16]: electronic excitations become delocalized with increasing size (generation) of the supermolecule. This experimental evidence comes from the study of dendrimer absorption spectra, which clearly shows that the first absorption peak for the compact family remains constant at a given wave length, while in the extended family this wave length decreases with increasing size. In other words, in extended dendrimers the gap for excitations from the ground state to the first excited states tends to close while it remains constant in compact dendrimers. Thus, there is experimental evidence for the following scenario:

$$\begin{aligned} \text{Compact Dendrimers} &\longleftrightarrow \text{Gapped Spectrum} \\ \text{Extended Dendrimers} &\longleftrightarrow \text{Gapless Spectrum} \end{aligned} \quad (4)$$

A complete *ab initio* computation of the electronic properties in these two families of dendrimers would require to include many different effects and a truly many-body model for these supermolecules. However, recently a very simple phenomenological model of one-exciton processes has been proposed by Harigaya [22, 23, 24] which produces good fits for the experimental absorption peaks in extended dendrimers.

In this paper our aim is to propose the density matrix renormalization group (DMRG) method as a good computational tool for dealing with one-exciton process in the presence of disorder. This method allows us to perform an exhaustive study of excitons in the Harigaya model to be explained below, for both families of dendrimers.

Our studies are theoretical, we consider dendrimers as a useful model for investigating the dependence of physical properties on molecular size and topology. This paper is organized as follows: in Sect. II we introduce a simple Frenkel Hamiltonian describing exciton processes and concentrate in one-exciton approximations using a recently introduced model Hamiltonian; in Sect. III we propose the DMRG method as an appropriate computation method for excitons with disorder in extended and compact dendrimers, and we present our numerical results in a variety of situations with different numbers of generations g and wedges w . Sect. IV is devoted to conclusions and future prospects.

II. EXCITONS IN DENDRIMERS

A consequence of the aforementioned experimental studies [16] is that the family of extended dendrimers can serve as artificial light-harvesting antennas. This has been demonstrated experimentally [18]. The light is harvested over a wide area on the surface of the dendrimer and funneled by dipole-dipole interactions to the single active site at the focal point where energy conversion takes place. Based on the optical spectra of the first absorption peak [16], Kopelman et al. conjectured that the electronic excitations in extended dendrimers are localized on the linear segments of the branched molecules. Theoretical studies have confirmed this fact showing that the relative motion of photogenerated electron-hole pairs (excitons) is confined to the various segments and energy-transfer may then be described by the Frenkel exciton model [19].

In the Frenkel exciton model, at each site of a lattice there is an active center modeled with a two-level system. At half-filling, there is an electron per site on average and in the absence of interactions among centers, the ground state $|GS\rangle$ is formed by putting each electron at

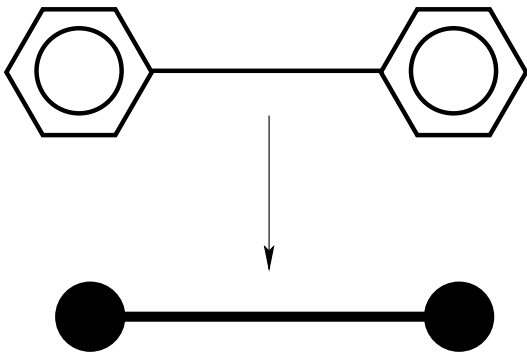


FIG. 4: Simplified treatment of the phenyl rings as single sites.

the corresponding ground states $|\text{vac}\rangle$ of the two-level systems, that is,

$$|\text{GS}\rangle = |\text{vac}\rangle_1 |\text{vac}\rangle_2 \dots |\text{vac}\rangle_N \quad (5)$$

A local excitation is formed by promoting one of the electrons at a given site to the first excited level $|\text{exc}\rangle$. This is a localized electron-hole pair that models an exciton. An example of this is the state

$$|\text{Ex}\rangle = |x\rangle = |\text{vac}\rangle_1 \dots |\text{exc}\rangle_x \dots |\text{vac}\rangle_N. \quad (6)$$

Let us introduce fermionic creation and annihilation operators $c_{i,\alpha}^\dagger, c_{i,\alpha}$ for these localized centers, where i denotes the lattice site and α is a label that stands for the energy levels: $\alpha = 0$ for $|\text{vac}\rangle$ and $\alpha = 1$ for $|\text{exc}\rangle$. Then, the localized energy levels can be represented as

$$\begin{aligned} |\text{vac}\rangle_i &= c_{i,0}^\dagger |0\rangle \\ |\text{exc}\rangle_i &= c_{i,1}^\dagger |0\rangle \end{aligned} \quad (7)$$

where $|0\rangle$ is the vacuum of the fermionic operators. The excitonic operator that creates one exciton from the localized ground state $|\text{vac}\rangle_i$ is denoted by b_i^\dagger and acts as follows

$$|\text{exc}\rangle_i = b_i^\dagger |\text{vac}\rangle_i, \text{ with } b_i^\dagger = c_{i,1}^\dagger c_{i,0}. \quad (8)$$

The excitonic operator b_i^\dagger creates a localized electron-hole pair at the site i and has bosonic character.

When interactions among centers are brought to the system, the interesting question is to see how one these excitons evolve under quantum fluctuations. A simple model for these interactions is presented in the Frenkel Hamiltonian, namely,

$$H = \sum_{i \in \Lambda} E_i b_i^\dagger b_i + \sum_{\langle i,j \rangle} J_{i,j} (b_i^\dagger b_j + b_j^\dagger b_i) \quad (9)$$

where E_i are chemical potentials that represent the energy gaps at each site of the lattice Λ and $J_{i,j}$ is a hopping integral for nearest-neighbour centers $\langle i,j \rangle$ that introduce interactions between the site centers [21]. The origin of these couplings is the residual electric dipole interactions between the molecules modeled by the active centers. It is assumed that this interactions are short-ranged. Their effect is to allow excitation transitions between nearest-neighbours sites.

Harigaya has recently proposed to study one-exciton processes in the family of extended dendrimers introducing off-diagonal disorder [22, 23, 24]. This simple model produces a good accurate phenomenological fit to the experimental data of the first absorption peak reported in [16]. Harigaya considers a first simplification of the molecular structure in extended dendrimers in order to make the analysis more tractable. This simplification amounts to replace the complicated phenyl rings by simple activation centers as depicted in Fig.4. A second approximation considered in [22, 23, 24] is to restrict the study to the one-exciton approximation within the Frenkel Hamiltonian (9) for excitons. We shall refer to this simple model based on these two approximations as the Harigaya model. A further assumption in this model is the presence of off-diagonal disorder.

To derive the one-exciton approximation of the Frenkel Hamiltonian (9) we project this Hamiltonian onto the Hilbert space of one-excited states (6) by considering a general superposition of localized excited states as follows

$$|\Psi_{\text{ex}}\rangle = \sum_{x \in \Lambda} C_x |x\rangle \quad (10)$$

where C_x are unknown amplitudes of the one-exciton states. Next, we set up the Schrödinger equation in this sector

$$H|\Psi_{\text{ex}}\rangle = \mathcal{E}_{\text{ex}}|\Psi_{\text{ex}}\rangle \quad (11)$$

The solution of this equation is equivalent to solving the Schrödinger equation for an associated one-body Hamiltonian $H_{1\text{ex}}$ that takes the following form

$$H_{1\text{ex}} = \sum_{i \in \Lambda} E_i |i\rangle \langle i| + \sum_{\langle i,j \rangle} (J_{i,j} |i\rangle \langle j| + \text{h.c.}) \quad (12)$$

where $|i\rangle$ are one-particle states representing an exciton state at site i . That is, an onsite exciton state is assigned to each phenyl ring (see Fig.3 and Fig.4).

In extended dendrimers, interaction strengths between neighbouring dipole moments may vary among position of dipole pairs. In the Harigaya model it is assumed that they are randomly distributed and the following Gaussian distribution function is chosen for the coupling strenghts

$$P(J_{i,j}) = \frac{1}{\sqrt{2\pi}J} e^{-\frac{1}{2}(\frac{J_{i,j}}{J})^2} \quad (13)$$

where J is the standard deviation of the interaction and the mean value of the interaction is taken as zero. Further, the excitation energies E_i are also assumed to be uniformly distributed

$$E_i = E, \quad \forall i. \quad (14)$$

Thus, the two adjustable parameters of the model are E and J . The former specifies the central energy position of excitons in the optical spectra. According to [22, 23, 24], we shall take the values of these parameters as $E = 37200\text{cm}^{-1}$ and $J = 3552\text{cm}^{-1}$, which were found to give the best fit to the experiments [16].

The diagonalization of (12) under these assumptions gives the energies of one excitation states measured from the ground state. The energy position of the optical absorption edge is always given by the lowest eigenvalue because the state with the lowest energy is always allowed for dipole transition from the ground state [22, 23, 24]. Thus, the values of the absorption edge E_{ab} (energy of the lowest optical excitation) for the family of extended dendrimers is computed as

$$E_{\text{ab}} = E - \langle e_0 \rangle J \quad (15)$$

where $\langle e_0 \rangle$ is the average of the ground state energies e_0 obtained by diagonalization and sampling of the one-exciton Hamiltonian in eq. (12).

To solve this model of stochastic fluctuations in the Hamiltonian matrix elements that simulates the random distribution of couplings, in [22, 23, 24] an exact diagonalization procedure was employed for a sampling of 10000 realizations. This was carried out up to the fifth generation of extended dendrimers which has 127 sites.

As in the computation of the first peak of the absorption spectra only the computation of the ground state of (12) matters, then it is clear that using an exact diagonalization method for solving a 127×127 matrix a number of 10000 times implies a waste of computer resources. Of all the over hundred eigenvalues, only one is needed. Thus, it would be more convenient to have a method that targets only the desired state with the same accuracy as the exact diagonalization method while not having to compute the remaining states. In next section we shall compute this absorption peak using the density matrix renormalization group method [25], [26], [27].

III. DMRG FOR EXCITONS: RESULTS

We propose to use the DMRG method as explained in [28] for the computation of one-exciton problems with off-diagonal disorder. This method has been used to compute with high accuracy the low lying energy states in quantum mechanical problems [29], not only in one dimensional lattices but also in two and three dimensions

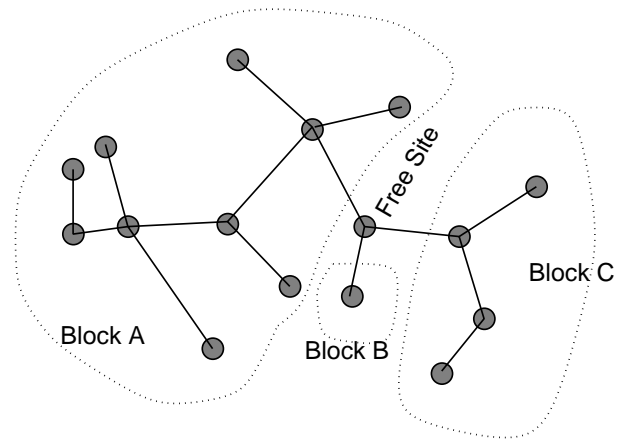


FIG. 5: Superblock decomposition of the lattice associated to a general tree graph (no cycles allowed). The free site denotes the probing site \bullet in the block splitting ABC \bullet .

[30]. The advantages of this quantum mechanical DMRG (QM-DMRG) over exact diagonalization models in one-exciton calculation are the following:

1. It is possible to reach lattice sizes that are out of the reach for exact diagonalization techniques, while keeping the same degree of accuracy in the determination of energies and wavefunctions.
2. It is possible to save both CPU time and space for the computations in each sampling. This is specially interesting when the number of samplings N_s is a large number.

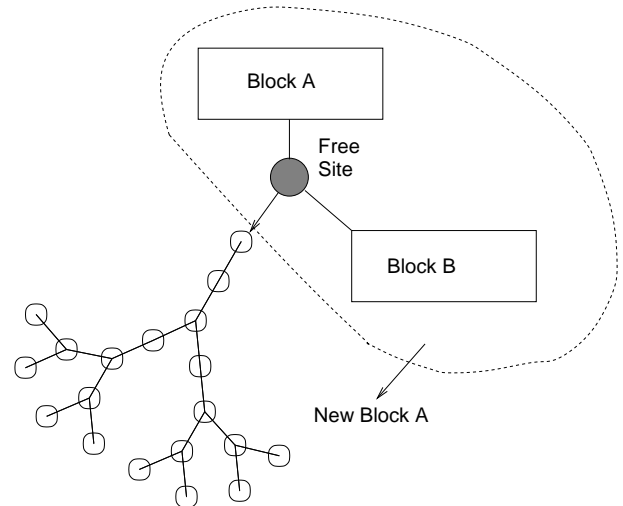


FIG. 6: Schematic representation of the sweeping process in the DMRG process for dendrimers. The free site is at a site with coordination number $c = 3$.

These properties make the QM-DMRG method specially well-suited for excitonic calculations in dimensions

higher than one when computation means due to disorder and connectivity become quite demanding.

We have tested this proposal in the interesting case of extended and compact dendrimers. With this method we can increase the number of generations g for each dendrimer family to sizes not reachable with other methods.

We shall not dwell upon all the details of the QM-DMRG formulation that can be found in [28, 29, 30], but instead we shall stress the main peculiarities of the method when applied to extended and compact dendrimers.

A DMRG for Dendrimer Lattices

For the sake of concreteness, we shall make the discussion in terms of dendrimers with a fixed number of wedges $w = 3$ and connectivity $c = 3$, motivated by the Harigaya model, but the method is equally applicable to a generic tree graph. Later, we shall present results when the number of wedges is different ($w \neq 3$).

In the standard formulation of the DMRG, the whole lattice also called *universe* \mathcal{U} or superblock (SB) is split into left (B_L) and right (B_R) blocks according to the decomposition: $\mathcal{U} = B_L \bullet B_R$ or $\mathcal{U} = B_L \bullet \bullet B_R$. The blocks describe the degrees of freedom of the system and the environment, which can be represented either by B_L or B_R depending on which stage of the RG-sweeping process we are. In the case of dendrimers, we find more appropriate to use the first decomposition based on one site, $\mathcal{U} = B_L \bullet B_R$. The single lattice site \bullet connects the two blocks and serve as a *probe* to test the reaction of the system degrees of freedom to the coupling to the rest of the environment. This probing site is a movable site that runs all over the lattice during the sweeping process.

Let us introduce the following notation for the Hamiltonian matrix elements in (12):

$$H_{\mathbf{i},\mathbf{j}} = \begin{cases} E & \mathbf{i} = \mathbf{j} \\ J & \|\mathbf{i} - \mathbf{j}\| = 1 \\ 0 & \text{otherwise;} \end{cases} \quad (16)$$

where \mathbf{i}, \mathbf{j} are vectors of integer components in a dendrimer lattice. We may use a binary notation for labeling these sites.

Although the planar dendrimer lattice extends all over the plane, there is a distinctive feature that makes it closer to a one single chain. Namely, given any two points, there exists a unique path joining them, unlike a real two-dimensional lattice like the square lattice. This characteristic is reminiscent of the left-right directions in one-dimensional chains and it is the basis for trying an application of DMRG here [30]. Next we briefly describe the several ingredients entering in the application of DMRG to dendrimer lattices.

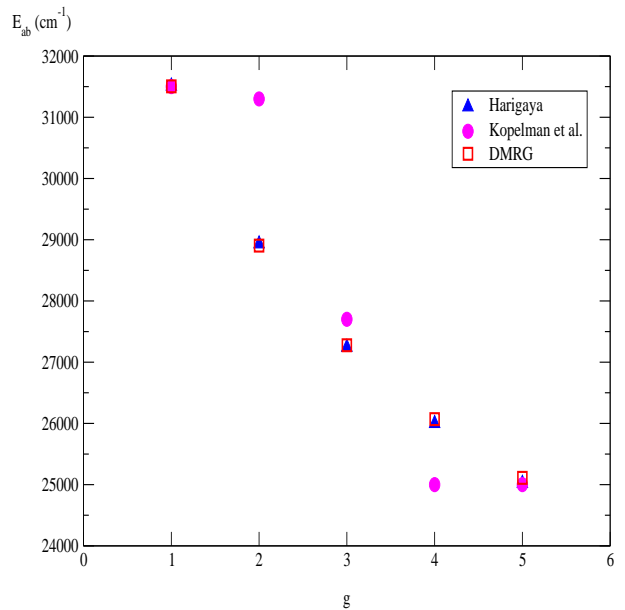


FIG. 7: Results for the first absorption peak E_{ab} as in (15) for extended dendrimers versus the generation number g . Two numerical methods are compared with the experimental results of Kopelman et al. [16]: DMRG (ours) and ED (Harigaya [22]).

1 Superblock Decomposition of the Dendrimer

The standard DMRG decomposition of the original lattice to perform the truncation/renormalization process is $\mathcal{U} = B_l^L \bullet \bullet B_{N-l-2}^R$ where the subscripts l and $N-l-2$ denote the number of sites inside each left and right blocks such that their sum - plus two - equals the total number of lattice sites N . The index l denotes the iteration step of the RG process. This decomposition applies both to one-dimensional lattices as well as higher dimensional cases [30].

In our case, for a generic dendrimer with a number w of wedges and sites with connectivity c , we use a superblock decomposition as follows

$$\mathcal{U} = B_1(l)B_2(l) \dots B_c(l)\bullet_l, \quad (17)$$

where the probing site is joint to the wedge-blocks (see Fig.5) and it is a movable point that traverses the dendrimer lattice as the sweeping process takes places. We denote it as a free point in Fig.5 and it is a generic point of the lattice for a given RG-step l , not always the focal point at the core. This decomposition is generic of a tree graph with no cycles and the DMRG decomposition is applicable with generality to any graph, as shown in Fig.5.

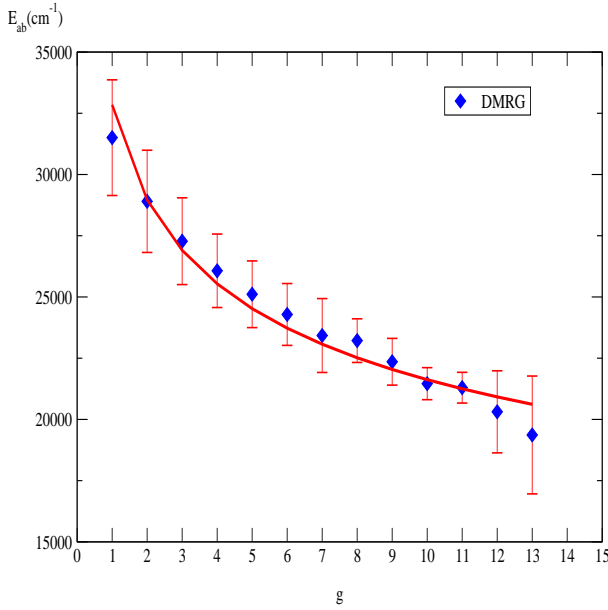


FIG. 8: DMRG results for the first absorption peak E_{ab} (15) in extended dendrimers versus the generation number g [31].

2 Wave-Function Variational Ansatz

Let us assume that the total number of states that we want to keep during the truncation/renormalization process is N_E , which includes the GS and $N_E - 1$ excited states. These are the targeted states and we are considering the more general case of finding not only the GS but also a few of the low lying excited states. Although this is not necessary for the one-exciton model that we are considering here, however we want to show that the method is powerful enough so as to handle more general situations.

The superblock decomposition of the lattice in turn induces a decomposition of the wave-function of the targeted states associated to the blocks and the free site. Let us assume extended and compact dendrimers with a generic value of w , then the superblock wave-function $\Psi_l(\mathbf{n})$ at RG-step l and lattice point \mathbf{n} is split into the following four pieces when the connectivity is $c = 3$ (17):

$$\Psi_l(\mathbf{n}) = \begin{cases} \sum_{\alpha=1}^{N_E} a_{\alpha} L_1^{\alpha}(\mathbf{n}; l) & \mathbf{n} \in B_1(l) \\ \sum_{\alpha=1}^{N_E} a_{N_E+\alpha} L_2^{\alpha}(\mathbf{n}; l) & \mathbf{n} \in B_2(l) \\ \sum_{\alpha=1}^{N_E} a_{2N_E+\alpha} L_3^{\alpha}(\mathbf{n}; l) & \mathbf{n} \in B_3(l) \\ a_{3N_E+1} & \mathbf{n} = \bullet_l \end{cases} \quad (18)$$

where \bullet_l denote the free point in Figs.5,6 connecting the blocks $B_c(l)$, $c = 1, 2, 3$; $\{L_c^{\alpha}(\mathbf{n}; l)\}_{\alpha=1}^{N_E}$, $c = 1, 2, 3$ are orthonormal basis of states describing the degrees of freedom in the wedge-blocks, i.e.,

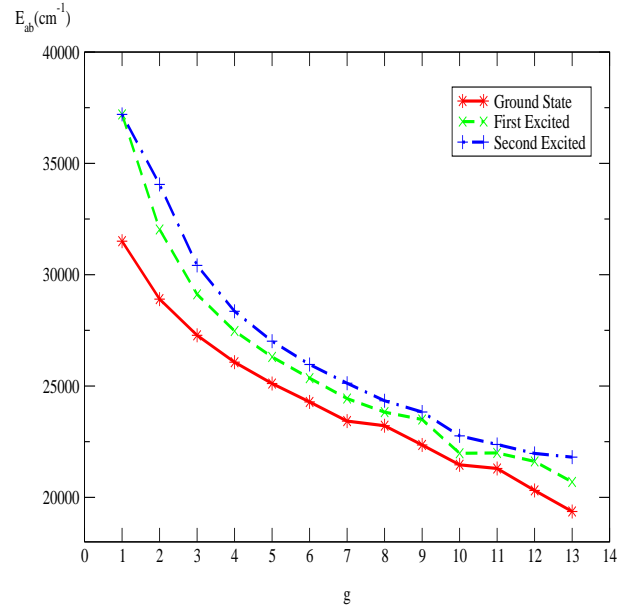


FIG. 9: DMRG results for the absorption peaks E_{ab} (15) in extended dendrimers (vertical versus the generation number g). They corresponds to the ground state and two excited states.

$$\langle L_c^{\alpha}(l) | L_{c'}^{\beta}(l) \rangle = \delta_{\alpha,\beta} \delta_{c,c'} \quad (19)$$

and the free unknown coefficients $\{a_{\alpha}\}_{\alpha=1}^{3N_E+1}$ at this l -stage will be determined later on by means of a diagonalization/truncation process defining the renormalization. They are normalized as

$$\|\mathbf{a}\|^2 = \sum_{\alpha=1}^{3N_E+1} a_{\alpha}^2 = 1 \quad (20)$$

In a generic case of a dendrimer with w wedges, there will be a number of blocks c at each stage l of the DMRG, and a number of $cN_E + 1$ variational a -parameters. For compact dendrimers with $w = 3$, all ansatz are like in (18) for every site. However, for extended dendrimers with $w = 3$ we have to distinguish two types of sites, those with $c = 2$ and those with $c = 2$ (see Fig. 3) In this case we need to use another ansatz like in (18) for only two blocks in (17) when dealing with sites of connectivity $c = 2$.

3 Superblock Hamiltonians

The dimensionality of these SB Hamiltonians follows from the wavefunction in (18), and it is much smaller than that of the original Hamiltonian (16). This makes their diagonalization something much less demanding

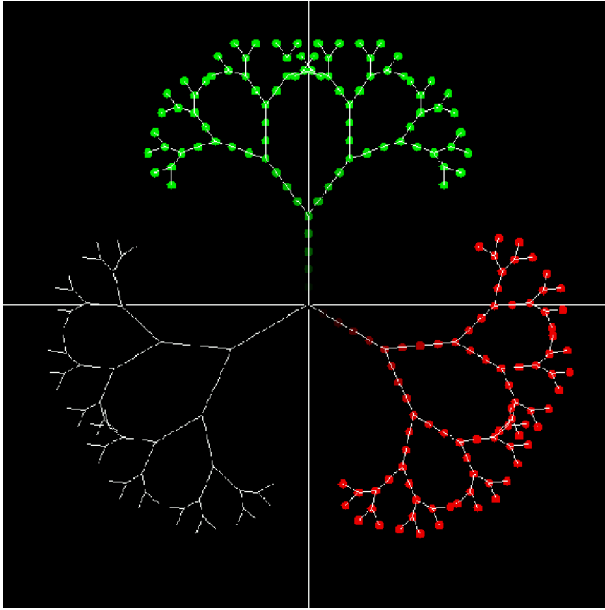


FIG. 10: Pictorial representation of the DMRG wavefunction for one excited state in an extended dendrimer with generation $g = 7$. The two colors denote positive and negative values of the state coefficients and their size are proportional to their normalized values.

than diagonalizing the whole Hamiltonian. The dimension of H_{SB} depends on the number of targeted states. In the version of the DMRG we are using here, this dimension is $(3N_E + 1) \times (3N_E + 1)$ for both families of dendrimers. For example, when the connectivity of a given site is $c = 3$ (where the free site (see Fig.5 6) lies at a given DMRG-step), then the SB Hamiltonian reads as follows

$$H_{SB}(l) = \begin{pmatrix} H_1(l) & 0 & 0 & v_1(l) \\ 0 & H_2(l) & 0 & v_2(l) \\ 0 & 0 & H_3(l) & v_3(l) \\ v_1^\dagger(l) & v_2^\dagger(l) & v_3^\dagger(l) & H_{\bullet_l, \bullet_l} \end{pmatrix} \quad (21)$$

where $H_c(l)$, $c = 1, 2, 3$ are the block Hamiltonians for each block in the DMRG decomposition of the lattice (see Fig.5,6) with dimensions $N_E \times N_E$, namely,

$$H_c^{\alpha, \beta} = \langle L_c^\alpha | H | L_c^\beta \rangle, \quad c = 1, 2, 3; \quad (22)$$

while H_{\bullet_l, \bullet_l} denotes the value of the original Hamiltonian (16) at the free site \bullet_l and the column vectors $v_c(l)$, $c = 1, 2, 3$ with dimension $N_E \times 1$ corresponds to the interactions between the blocks and the free site. Their values depend on the DMRG-step l and constantly updated through the RG process. The zeroes in (21) reflect the short-range structure of (16).

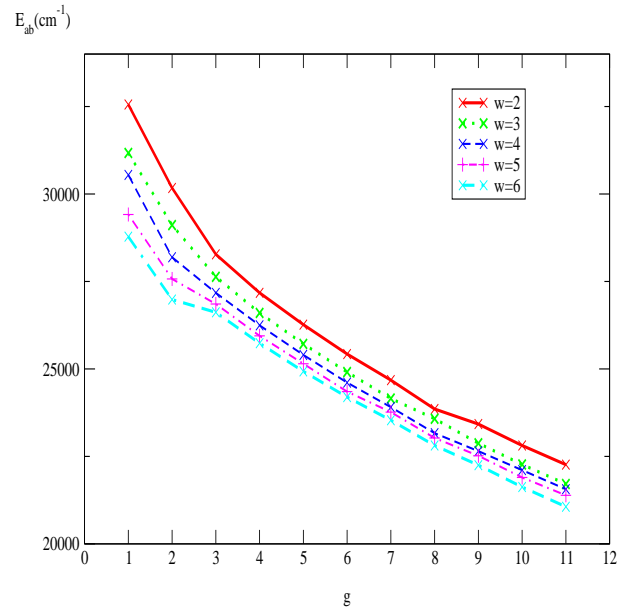


FIG. 11: DMRG results for the first absorption peak E_{ab} (15) in extended dendrimers versus the generation number g and with varying number of wedges w .

4 Truncation of Hilbert Space and Renormalization

The next step is the diagonalization of the superblock Hamiltonians in order to obtain the wave functions of the N_E targeted states and their energies. The free parameters \mathbf{a} are then constructed out of the components of the targeted wave functions. With this information we can perform the projection of the wave functions onto the several blocks as well as the renormalization of the matrix elements of the superblock Hamiltonian.

Let us denote the variational parameters by the set $\{\mathbf{a}_1^i, \mathbf{a}_2^i, \mathbf{a}_3^i, a_{\bullet_l}^i\}_{i=1}^{N_E}$, where \mathbf{a}_c^i , $c = 1, 2, 3$ are N_E -dimensional vectors. Assuming that we have three blocks ($c = 3$), then the truncation of the Hilbert space is performed by the projection of the superblock wave-function (18) onto the blocks formed by two out of three possible blocks plus the free site. For definiteness, let us assume that we are renormalizing blocks $B_1(l), B_2(l)$ at a given DMRG-step l , while the remaining block $B_3(l)$ is not directly renormalized but only updated through the values taken from a previous DMRG-step. Then, the projection onto the blocks $B_1(l), B_2(l)$ is given by

$$\mathbf{a}^i = \begin{pmatrix} \mathbf{a}_1^i \\ \mathbf{a}_2^i \\ \mathbf{a}_3^i \\ a_{\bullet_l}^i \end{pmatrix} \longrightarrow \begin{pmatrix} \mathbf{a}_1^i \\ \mathbf{a}_2^i \\ a_{\bullet_l}^i \end{pmatrix} \quad (23)$$

The projected wave functions in the RHS of (23) must be orthonormalized using a Gram-Schmidt method. They will become the new wave functions of the renormalized blocks B'_1, B'_2 . More explicitly, we have

$$\begin{pmatrix} \mathbf{a}_1^{i_i} \\ \mathbf{a}_2^{i_i} \\ a_{\bullet_i}^{i_i} \end{pmatrix} = \sum_j \mathcal{O}_{ij}^{(12)} \begin{pmatrix} \mathbf{a}_1^j \\ \mathbf{a}_2^j \\ \mathbf{a}_{\bullet_i}^j \end{pmatrix} \quad (24)$$

where $\mathcal{O}^{(1)}$ is the orthonormalization matrix. The new wave functions $L_1^{i_i}(l+1)$ for the renormalized block B_1' to be constructed in the next RG-step $l+1$ are given by

$$L_1^{i_i}(\mathbf{n}; l+1) = \begin{cases} \sum_{\alpha} a_{1,\alpha}^{i_i} L_1^{\alpha}(\mathbf{n}; l) & \mathbf{n} \in B_1(l) \\ \sum_{\alpha} a_{2,\alpha}^{i_i} L_2^{\alpha}(\mathbf{n}; l) & \mathbf{n} \in B_2(l) \\ a_{\bullet_i}^{i_i} & \mathbf{n} = \bullet_l \end{cases} \quad (25)$$

After the truncation process we need to renormalize (update) the different matrix elements of the superblock Hamiltonian (21). For the blocks B_1', B_2' we have

$$H_1'(l+1) = A'^{\dagger} \begin{pmatrix} H_1(l) & 0 & v_1(l) \\ 0 & H_1(l) & v_2(l) \\ v_1^{\dagger}(l) & v_2^{\dagger}(l) & H_{\bullet_i, \bullet_i} \end{pmatrix} A' \quad (26)$$

$$A' = \begin{pmatrix} \mathbf{a}_1^{i_1} & \dots & \mathbf{a}_1^{i_{NE}} \\ \mathbf{a}_2^{i_1} & \dots & \mathbf{a}_2^{i_{NE}} \\ a_{\bullet_i}^{i_1} & \dots & a_{\bullet_i}^{i_{NE}} \end{pmatrix} \quad (27)$$

These considerations for the renormalization of blocks $B_1(l), B_2(l)$ are generic and they equally apply to the other pairs of blocks. Moreover, when the free site is placed at a lattice site with connectivity $c=2$, then the renormalization is simplified for then there are only 2 blocks and the RG process is similar to a one-dimensional DMRG step, with a lattice decomposition of the type $B \bullet B$.

5 Sweeping Dendrimers

This part of the finite-size DMRG method corresponds to moving the free site in Fig. 6 throughout the lattice at each step of the RG process and updating the content of the blocks in the DMRG decomposition of the lattice following the previous renormalization prescriptions. The sweeping process is responsible for the convergence of the method: the sweeping continues until the energy values of the intermediate diagonalizations achieve a desired prescribed precision.

During a generic DMRG sweep, the free site starts at the focal point and then moves first through the sites in wedge $w=1$, next the sites of $w=2$ are visited and so on and so forth with the rest of the wedges until the free site returns to the focal point. The sweeping process needs a first input called warm-up in order to start up. In the case of dendrimers we find useful to do it with a simple

block renormalization group method (BRG). This means that the dendrimer lattice is decomposed in blocks. The blocks in this BRG are formed with 3 sites, one of these sites is the father and the other two are children. The first step of this BRG starts with a blocking for the outermost sites located at the surface of the dendrimer, namely, the last and next-to-last generations. During the following BRG-steps, the dendrimer lattice is reconstructed from the outside to the focal point located at the core. At this moment, the warm-up process is completed. Interestingly enough, this form of doing the warm-up in the DMRG for dendrimers is similar to one of the actual methods of chemical synthesization: the convergent method [15].

B Numerical Results

Let us start presenting our numerical results for the family of extended dendrimers. Our main purpose is to show the capabilities of the DMRG method when dealing with one-exciton problems in the presence of disorder such the case of the Harigaya model that we have taken as our model Hamiltonian (12,13).

We have targeted a number $N_E = 3$ of states that include the ground state plus two excited states. The convergence criterion used is to sweep until a precision (relative error) of 10^{-10} is achieved in all the eigenvalues. We find that the degree of convergence with our DMRG is very fast. For instance, the number of sweeps needed to achieve this accuracy is always lower than 4. The number of samples is also $N_S = 10000$ as in [22, 23, 24]. The corresponding CPU times are also very small as compared with exact diagonalization times. For example, for the sampling considered here a typical time for the dendrimers with higher generation number is around 900 s [32]. We start with the number of wedges $w=3$.

In Fig. 7 we present the results for the first absorption peak E_{ab} (15) in extended dendrimers versus the generation number g until a value of 7. The energies are measured in cm^{-1} . Here we are doing two types of comparisons. Firstly, we are comparing our DMRG results with the exact diagonalization results (ED) of Harigaya up to 5 generations. We clearly see that there is an overlapping of both results and furthermore, we can go easily to higher generations. Secondly, we must note in passing that there is qualitative agreement between the experimental results of Kopelman et al. [16] and those of Harigaya's, although a better quantitative matching would be desirable.

We have been able to reach a generation number of $g=13$ without using big computer facilities [32] as shown in Fig. 8. The vertical lines at each result in this figure are error bars due to statistical fluctuations in the sampling. It is apparent from these results that there is a decreasing of the absorption peak as the generation number increases, in qualitative agreement with the experi-

mental results of Kopelman et al. [16]. Although in [16] only extended and compact dendrimers up to $g = 5$ were considered, it has been possible experimentally to reach higher generation numbers in a variety of dendrimers of different compositions. In our case, we are also interested in studying theoretically the behaviour with g of physical properties in dendrimers. As it happens, due to the exponential growth of the number of sites with g , the dendrimer tends to reach an upper generation limit because the surface groups become densely packed. This is known as the “de Gennes dense packing”. For some dendrimers, this limit has been found around $g = 10$ to $g = 12$.

As a result of having this many values we can make a polynomial fit to estimate the degree of this slowing down. We find that the following scaling law with the generation number g

$$E_{ab}^e = 32000 - C_e g^{\alpha_e} \text{ cm}^{-1}, \quad (28)$$

fits well the numerical data with the values $C_e = 2020 \pm 200 \text{ cm}^{-1}$ and the scaling exponent $\alpha_e = 0.71 \pm 0.04$. The continuous line in Fig. 8 gives the fitting in (28).

As we are interested in the performance of the DMRG method when dealing with excitons, we also plot two byproducts of our numerical calculations. On one hand, in Fig. 9 we present the results for the absorption peaks E_{ab} (15) corresponding not only to the ground state, but also to the lowest two excited states. They are computed simultaneously when targeting $N_E = 3$ states. We see that all of these states have decreasing energies as the generation number increase. Within the approximations of the Harigaya model, this is an indication that these lowest lying states are delocalized. On the other hand, in Fig. 10 we show a plot of the wavefunction corresponding to an excited state for a generation number of $g = 7$. This is because the DMRG not only gives energies but also computes the corresponding states. In this pictorial view of the excited state in the extended dendrimer, each circle has a size proportional to the value of the coefficient of the normalized wavefunction and the two colors corresponds to positive and negative values. Notice that in one of the wedges the state has vanishing contributions.

So far we have considered the number of wedges fixed to $w = 3$, following the experimental studies in [16] and the computations in [22, 23, 24]. However, as for several types of dendrimers the number of wedges achieved experimentally can be different than this number [33, 34, 35], we have also applied our DMRG studies to deal with extended dendrimers with variable number of wedges ranging from $w = 2$ to $w = 6$ as shown in Fig. 11. In this figure we present the first absorption peaks E_{ab} (15) as a function of g and with varying number w . It is clearly seen that the effect of increasing w is to lower the energy peaks for any generation number (there are no level crossings). For a fixed value of w , the behaviour of the peaks are all qualitatively similar.

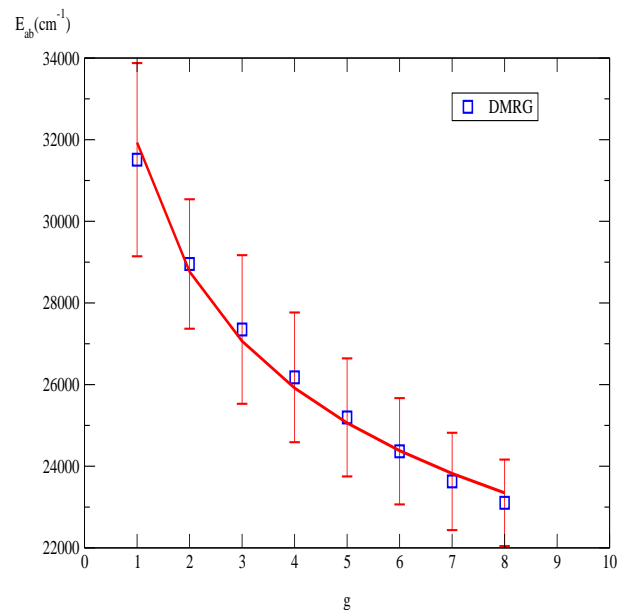


FIG. 12: Results for the first absorption peak E_{ab} (15) using DMRG in compact dendrimers versus the generation number g [31].

For the sake of completeness, we have also performed a DMRG study in the family of compact dendrimers with a fixed number of wedges $w = 3$ using the Harigaya model (12),(13). We plot the first absorption peak E_{ab} (15) as a function of g up to 8, with the corresponding error bars. From this figure it is shown that the energy peaks also decrease with increasing sizes for this family of dendrimers and thus the Harigaya model is not able to predict the correct experimental data in [16]. We can make a polynomial fit to estimate again the degree of this decay. We find that the following scaling law

$$E_{ab}^c = 32000 - C_c g^{\alpha_c} \text{ cm}^{-1}, \quad (29)$$

fits very well the numerical data with the values $C_c = 3190 \pm 120 \text{ cm}^{-1}$ and the scaling exponent $\alpha_c = 0.54 \pm 0.02$. The continuous line in Fig. 12 gives the fitting in (29). Thus, the only difference that we can capture between both families of dendrimers is the fact that the scaling exponent α_e in the extended dendrimers is bigger than α_c for the compact ones.

IV. CONCLUSIONS AND PROSPECTS

The field of dendrimers has become very active in Chemistry during the last decade due to their many possible applications explained in the introduction and we believe that there are open physical problems and new physics so as to make also an entrance in condensed matter also.

In this work we have been interested in the one-exciton processes pertaining to the application of extended dendrimers as light-harvesting molecules, i.e., molecular antennas. Our main contribution is to introduce the DMRG method as a very appropriate computational tool for one-exciton approximations with off-diagonal disorder. This is because the renormalization/truncation process in a DMRG calculation is more efficient than the exact diagonalization method if we are only interested in the low-lying states of the model Hamiltonian. The gain of the DMRG method is more pronounced when a large number of diagonalizations are needed such the large samplings typical of disorder problems with excitons.

We have shown the potentialities of the DMRG method in the field of excitons with disorder by computing a variety of dendrimer configurations with a variable number of generations g and wedges w (1). In all our computations we reproduce the exact results for low generation number and further, we can increase g without much computational effort to numbers that become unreachable for exact diagonalizations techniques (ED). Thus we propose to substitute these ED methods by the DMRG in situations like two-dimensional square lattices where the computation of one-exciton results with disorder and long-range interactions becomes very demanding for ED methods. For instance, we have computed lattices with a number of 36823 sites in the case of extended dendrimers, just to give an example of the sizes that can be reached with DMRG.

One of the open questions in the field of extended/compact dendrimers is the explanation of the scenario in (4) regarding the closing or not of the gap in the absorption spectrum using a more elaborate model Hamiltonian than the oversimplified Harigaya model [22, 23, 24]. It is plausible to think that a truly many-body Hamiltonian would be necessary in any attempt to address this issue. If we concentrate only in the electronic properties of these compounds, one possible candidate to describe the physics of multi-excitonic processes is a PPP (Pariser-Parr-Pople) Hamiltonian [6, 7, 8]. This type of Hamiltonian has been used with success in conjugated polymers of linear types and we believe that it could also be of use for conjugated polymer of dendrimer type. Another simpler candidate for a many-body Hamiltonian description of the gap spectrum in extended/compact dendrimers is the Frenkel Hamiltonian introduced in (9) that is more manageable for a first try than the PPP Hamiltonian. These types of studies are left for future work.

ACKNOWLEDGMENTS

We would like to thank K. Harigaya for reading a draft version of this work. This work has been partially supported by the Spanish grant PB98-0685.

REFERENCES

- [1] Dendrimer = dendrite + dimer. From the Greek word dendra = tree. Dendrites are the terminations of brain cells (neurons), while dimers are bonds (singlets).
- [2] D. A. Tomalia, P. R. Dvornic, *Nature* **372**, 617 (1994); R. F. Service, *Science* **267**, 458, (1995); J. Alper, *Chem. Ind.* 268, (1991).
- [3] G.R. Newkome, C.N. Moorefield, "Dendrimers" in *Comprehensive Supramolecular Chemistry*; Reinholdt, D. N., Ed.; Elsevier: New York, 1996; Vol. 10, Chapter 26.
- [4] G.R. Newkome, C.N. Moorefield, C. N.; F. Vögtle, *Perspectives*; VCH: Weinheim, Germany, 1996.
- [5] O.A. Matthews, A.N. Shipway, J.F. Stoddart, *Prog. Polym. Sci.* 1-56, (1998).
- [6] D. Baeriswyl, D.K. Campbell and S. Mazumdar, in *Conjugated Conducting Polymers*, edited by H. Kiess (Springer-Verlag, Heidelberg, 1992), pp 7-133.
- [7] S. Pleutin, E. Jeckelmann, M.A. Martin-Delgado, G. Sierra, "The Recurrent Variational Approach applied to the Electronic Structure of Conjugated Polymers", *Progress in Theoretical Chemistry and Physics*; cond-mat/9908062.
- [8] M.A. Martin-Delgado, G. Sierra, S. Pleutin, E. Jeckelmann, "Matrix Product Approach to Conjugated Polymers", *Phys. Rev. B* **61**, 1841 (2000); cond-mat/9908066.
- [9] C. J. Suckling, *J. Chem. Soc., Chem. Commun.*, 661, (1982).
- [10] J. A. Hyatt, *J. Org. Chem.* **43**, 1808-1811, (1978); F. Vögtle, E. Weber, *Angew. Chem. Int. Ed. Engl.* **13**, 814-815, (1974).
- [11] Y. Murakami, A. Nakano, K. Akiyoshi, K. Fukuya, *J. Chem. Soc., Perkin Trans 1*, 2800-2808 (1981).
- [12] E. Buhleier, W. Wehner, F. Vögtle, *Synthesis*, 155-158, (1978).
- [13] D.A. Tomalia et al., *Polym. J.* **17**, 117-132, (1985); D. A. Tomalia et al., *Macromolecules* **19**, 2466-2468, (1986). For an extensive review, see: D. A. Tomalia, A. M. Naylor, W. A. Goddard III, *Angew. Chem. Int. Ed. Engl.* **29**, 138-175, (1990).
- [14] R. G. Denkwalter, J. Kolc, W. J. Lukasavage, *US Pat.* **4**, 289, (1981).
- [15] C.J. Hawker, J.M. Frechet, *J. Am. Chem. Soc.* **112**, 7638-7647, (1990).
- [16] R. Kopelman, M. Shortreed, Z-Y. Shi, Z. Xu, J.S. Moore, A. Bar-Haim, J. Klafter, "Spectroscopy Evidence for Excitonic Localization in Fractal Antenna Supermolecules", *Phys. Rev. Lett.* **78** 1239, (1997).
- [17] J.F.G.A. Jansen, E.M.M. de Brabander-van den Berg, E.W. Meijer, *Science* **266**, 1226-1229 (1994).
- [18] C. Devadoss, P. Bharathi, and J. S. Moore, *J. Am. Chem. Sec.* **118**, 9635 (1996); M. Shortreed, Z-Y. Shi, and R. Kopelman, *Mole. Cryst. Liq. Cryst.* **28**, 95 (1996); M. R. Shortreed, S. F. Swallen, Z-Y. Shi,

- W. Tan, Z. Xec, C. Devadoss, J. S. Moore, and R. Kopelman, *J. Phys. Chem. B* **101**, 6318 (1997).
- [19] A. Bar-Haim, J. Klafter, and R. Kopelman, *J. Am. Chem. Soc.* **119**, 6197 (1997); A. Bar-Haim and J. Klafter, *J. Phys. Chem. B* **102**, 1662 (1998); A. Bar-Haim and J. Klafter, *J. of Luminescence* **76-77**, 197 (1998); A. Bar-Haim and J. Klafter, *J. Chem. Phys.* **109**, 5187 (1998).
- [20] S. Raychaudhuri, Y. Shapir, V. Chernyak, S. Mukamel, "Excitonic Funneling in Extended Dendrimers with Non-Linear and Random Potentials", *Phys. Rev. Lett.* **85**, 282 (2000).
- [21] The excitonic operators b_i are in fact hard-core bosons. The local states $|\text{vac}\rangle_i$, $|\text{exc}\rangle_i$ are in one-to-one correspondence with spin states $|-\rangle_i$, $|+\rangle_i$ and likewise, the operators b_i , b_i^\dagger and $b_i^\dagger b_i$ can be represented by Pauli matrices σ_i^- , σ_i^+ and $(\sigma_i^z + 1)/2$, respectively. Thus, the Hamiltonian (9) becomes the XY model with transverse couplings given by $J_{i,j}$ and external magnetic field given by E_i .
- [22] K. Harigaya, "Coupled exciton model with off-diagonal disorder for optical excitations in extended dendrimers" *Phys. Chem. Chem. Phys.* **1**, 1687 (1999).
- [23] K. Harigaya, "Optical excitations in diphenylacetylene based dendrimers studied by a coupled exciton model with off-diagonal disorder" *Int. J. Mod. Phys. B* **13** 2531, (1999).
- [24] K. Harigaya, "Optical Excitations in Fractal Antenna Supermolecules: Extended Dendrimers" in 4th Int. Symposium on Advanced Physical Fields: Quantum Phenomena in Advanced Materials at High Magnetic Fields.
- [25] S.R. White, *Phys. Rev. Lett.* **69**, 2863 (1992).
- [26] S.R. White, *Phys. Rev. B* **48**, 10345 (1993).
- [27] S.R. White and R. Noack, *Phys. Rev. Lett.* **68**, 3487, (1992).
- [28] M.A. Martin-Delgado, G. Sierra and R.M. Noack, *J. of Phys. A: Math. and Gen.* **32**, 6079 (1999).
- [29] M.A. Martin-Delgado and G. Sierra, *Phys. Rev. Lett.* **83**, 1514 (1999).
- [30] M.A. Martin-Delgado, J. Rodriguez-Laguna, G. Sierra; *Single-Block Renormalization Group: Quantum Mechanical Problems*, cond-mat/0009474 (2000).
- [31] The error bars for $g = 12, 13$ are bigger in these generations just because the sampling number is reduced, namely, $N_S = 100$.
- [32] We have used a personal computer with a Pentium III at 450 MHz.
- [33] J. M. J. Fréchet, *J. Am. Chem. Soc.* **112**, 7638-7647 (1990).
- [34] R. Roy, D. Zanini, S. J. Meunier, A. Romanowska, *J. Chem. Soc., Chem. Commun.* 1869-1872 (1993).
- [35] An example of a 4-lobule dendrimer is the Porphyrin-cored third generation dendrimer synthesized in P. J. Dandliker et al. *Angew. Chem. Int. Ed. Engl.* **33**, 1739-1742 (1994); H.-F. Chow et al., *Chem. Eur. J.* **2**, 1085-1091 (1996).